Alkane Retrievals from Lamont OK

Harrison A. Parker[1], Geoff C. Toon[2], Ariana Tribby[3], Debra Wunch[4], Coleen M. Roehl[1], Paul O. Wennberg[1,5]

[1]Division of Geological and Planetary Sciences, California Institute of Technology, Pasadena, CA, USA, [2]Jet Propulsion Laboratory, California Institute of Technology, Pasadena, CA 91109, USA, [3]Division of Chemistry and Chemical Engineering, California Institute of Technology, Pasadena, CA 91125, USA [4]Department of Physics, University of Toronto, Toronto, ON, Canada , [5]Division of Engineering and Applied Science, California Institute of Technology, Pasadena, CA, USA

Natural Gas Emissions

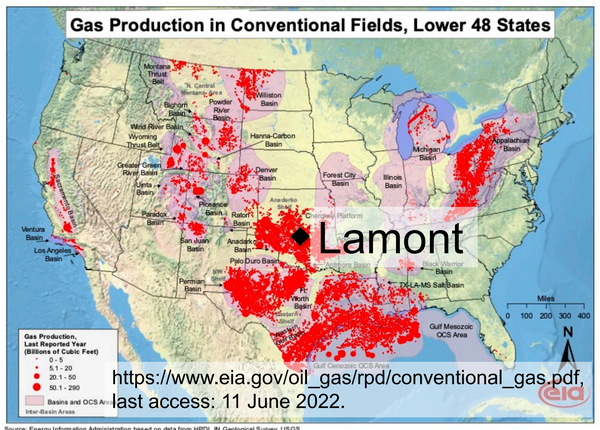

The Lamont, OK TCCON site is near the oil and natural gas production from the Anadarko Basin.

Oil and natural gas production has fugitive emissions composed of various hydrocarbons including large amounts of ethane (C_2H_6) and propane (C_3H_8).

Depending on the local composition of the gas and when leaks occur during processing, the ratio of C_3H_8 to C_2H_6 can serve as an identifier for the emissions.

Toon et al, 2021 used the MkIV interferometer to measure C_3H_8 in the 2967 cm^{-1} spectral window focused on its Q-branch absorption feature.

We retrieve XC_2H_6 and XC_3H_8 using the the 2976 and 2986 cm^{-1} spectral window for C_2H_6 and the same 2967 cm^{-1} spectral window as the MkIV for C_3H_8 using the Lamont, OK TCCON data.

Toon et al, 2021 suggests filtering the XC_3H_8 for data that has uncertainties less than 0.74 ppb and we use this filter for all the following data.

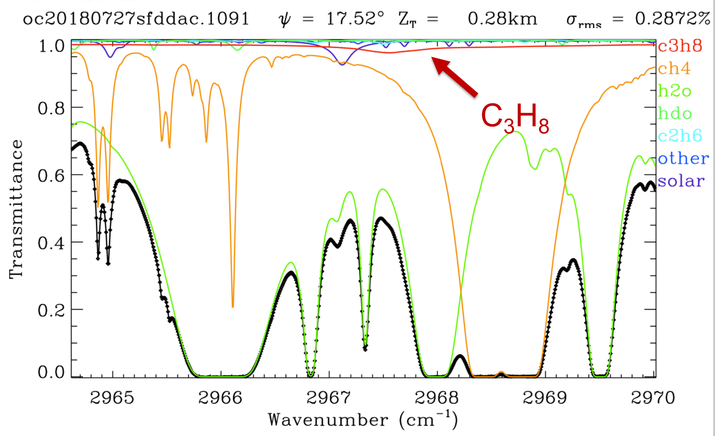

A Year of Data - 2018

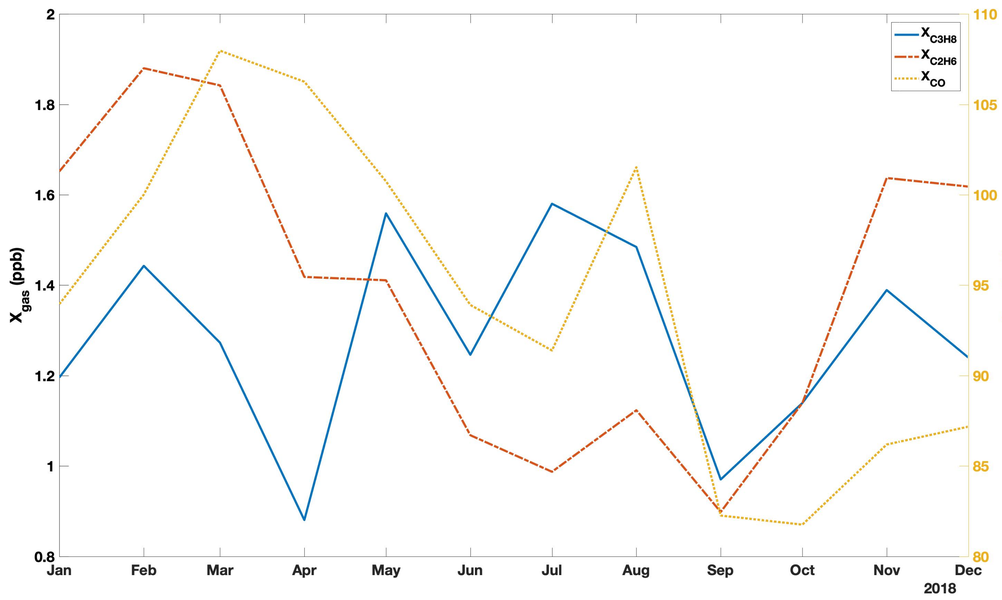

Monthly averages of XC_2H_6 (orange, left y-axis), XC_3H_8 (blue, left y-axis), and XCO (yellow, right y-axis) for 2018 show seasonal variations and loose correlations between all three variables.

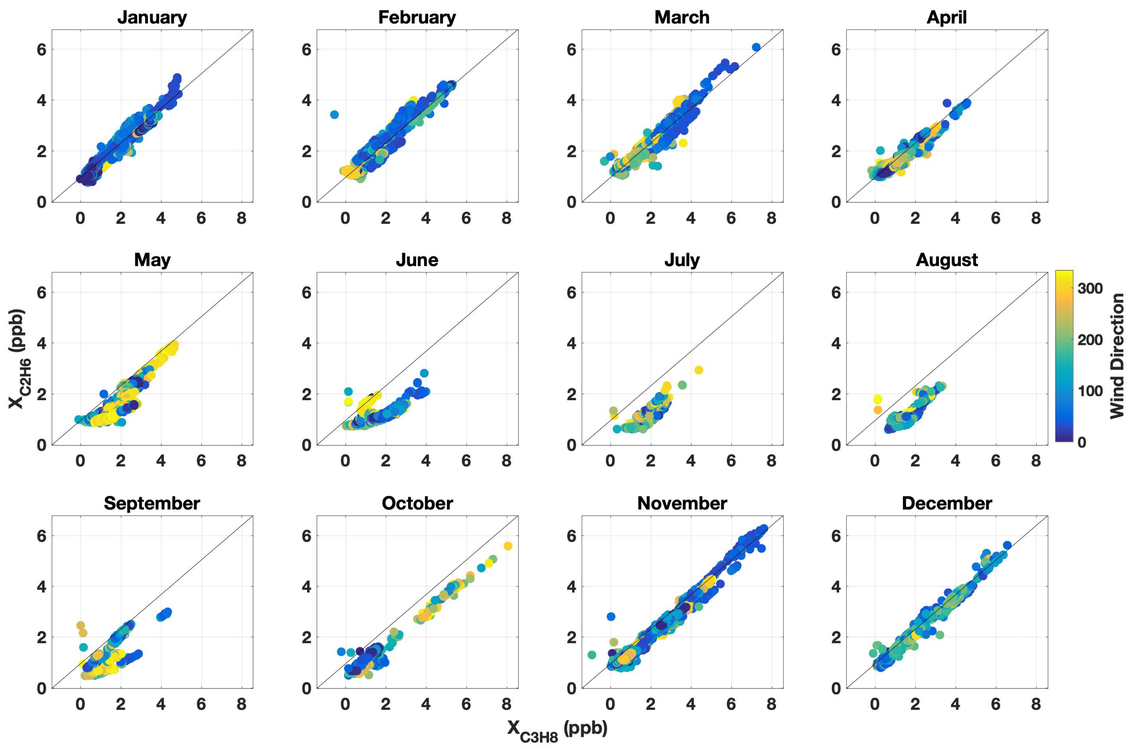

The monthly plots of the XC_2H_6 versus XC_3H_8 color coded by the wind direction at the surface show the consistency of the ratio between them from month to month and that the ratio holds across most months and observed wind directions. The black lines serve as references between plots and have no physical meaning.

Isolating Representative Data

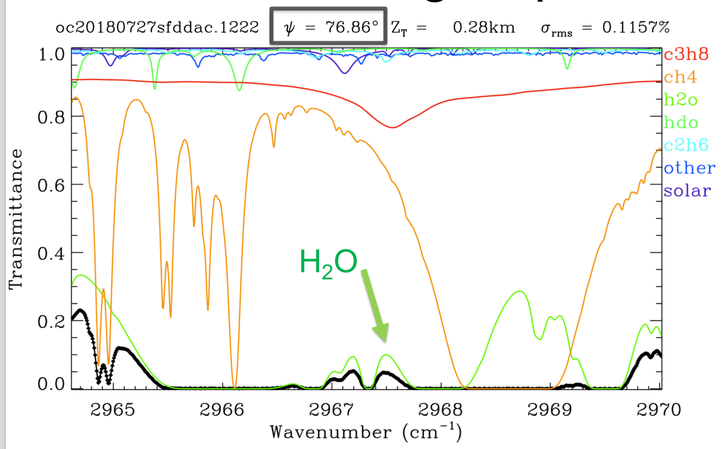

As Toon et al, 2021 discusses, the errors in the fit increase at higher airmasses due to signal saturation. These are largely caught by the error filter.

The main absorber in the XC_3H_8 spectral window is water which is a main cause of saturation and increases the errors of the fit.

Histograms of the data filtered by the errors show that the error filter is also excluding measurements made at high specific humidity.

We implement a filter based on surface specific humidity at an arbitrary level of 12 g/kg.

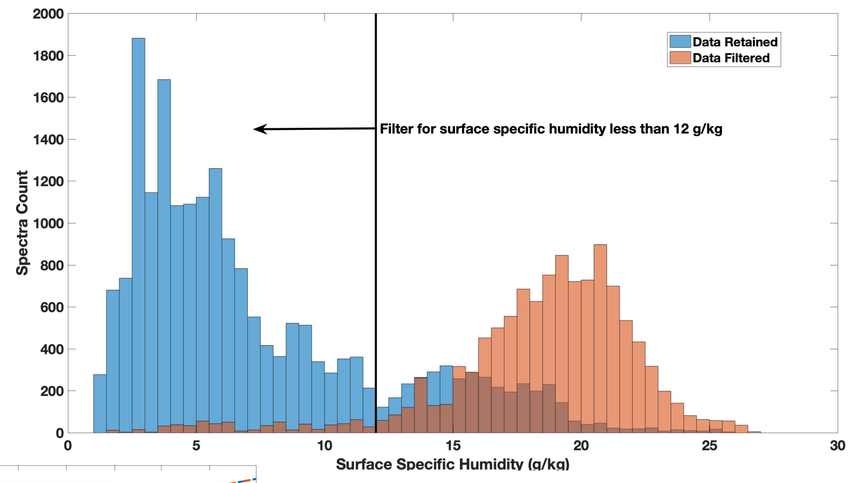

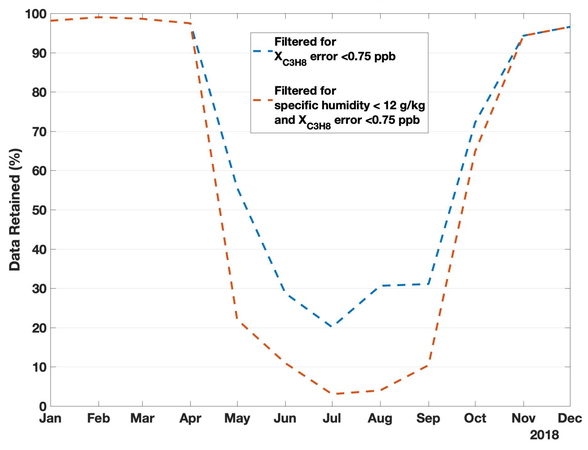

Filtering the data by the error threshold removes 36% of the data for 2018 but most data filtered is from the May to October time period.

Filtering the data by the error **and** the specific humidity removes 48% of the data which is still mostly from the May to October time period.

As a simple start, we also filter out months that have less than 50% of data remaining which are June, July, August and September using the error filters and the same in addition to May using the specific humidity filter.

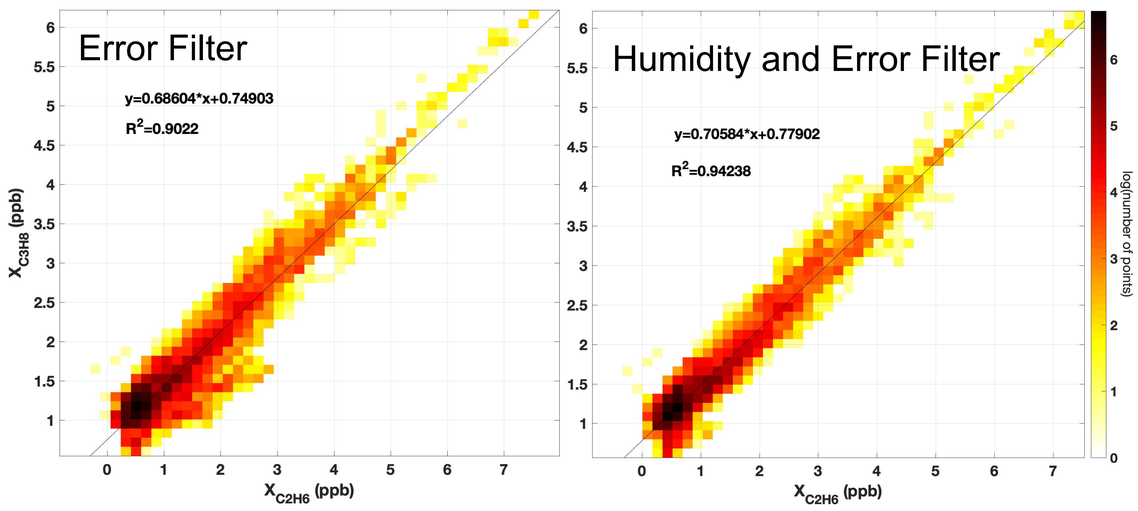

Filtering by specific humidity and removing the May data improves the fit between the XC_3H_8 and the XC_2H_6 by about 4%.

The slope of 0.706 from the fit is close to the observed in situ ratio range of XC_3H_8 / XC_2H_6 of 0.63 to 0.70 from NOAA Global Monitoring Lab surface flask measurements made between 2005 and 2018 although our measurements do not currently account for the averaging kernel effects.

The persistent ratio suggests a nearby, consistent emission source such as oil and gas emissions.

Future Directions

There are more elegant methods of filtering the data that we can explore, including using the slant water column instead of surface specific humidity.

The retrievals will benefit from improved prior profiles and the addition of the 2983 cm^{-1} window for the C_2H_6 measurement for the 2018 data and the rest of the Lamont site dataset.

If we can account for the averaging kernels, we could better assess the signal from the local emissions.

References

Toon, G. C., Blavier, J.-F. L., Sung, K., and Yu, K.: Spectrometric measurements of atmospheric propane (C3H8), Atmos. Chem. Phys., 21, 10727–10743, https://doi.org/10.5194/acp-21-10727-2021, 2021.

Tribby, A. L., Bois, J. S., Montzka, S. A., Atlas, E. L., Vimont, I., Lan, X., Tans, P. P., Elkins, J. W., Blake, D. R., and Wennberg, P. O.: Hydrocarbon Tracers Suggest Methane Emissions from Fossil Sources Occur Predominately Before Gas Processing and That Petroleum Plays Are a Significant Source, Environ. Sci. Technol., https://doi.org/10.1021/acs.est.2c00927, 2022.